MSS10, final version

Intersubband relaxation dynamics in semiconductor quantum structures

R. Bratschitsch, T. Müller, G. Strasser, and K. Unterrainer

Institut für Festkörperelektronik, Technische Universität Wien, A-1040 Wien, Austria

We monitor the temporal evolution of the electron population in the first and second subband of an undoped GaAs/AlGaAs asymmetric double quantum well after interband optical excitation by using an interband pump/intersubband probe technique. The spacing between the two subbands is smaller than the longitudinal optical phonon energy. We extract an intersubband lifetime of T_{21} = 100 ps and a recombination time of τ = 410 ps at an excitation density of $n_S = 8 \times 10^{10}$ cm^{-2}. Results from a simple rate equation model fit very well to our data.

PACS: 73.50.Gr, 78.47.+p, 07.57.-c

Keywords: intersubband, electron population, relaxation time, double quantum well

Rudolf Bratschitsch
Institut für Festkörperelektronik
TU Wien
Floragasse 7
A-1040 Wien
Tel: +43-1-58801-36228
Fax: +43-1-58801-36299
Email: Rudolf.Bratschitsch@tuwien.ac.at

The design of quantum cascade lasers [1] and other devices based on intersubband transitions [2,3] critically depends on the knowledge of the intersubband relaxation times.

A variety of techniques have been applied to measure the relaxation time T_{21} in modulation-doped [4-9] and undoped [10-13] structures with $E_{12} < \hbar\omega_{LO}$, leading to values of T_{21} between a few picoseconds and more than one nanosecond. This discrepancy has been explained by the strong dependence of the intersubband scattering rates on the excitation conditions.

We have developed a time-resolved interband pump/intersubband probe technique. In our experiment an interband pump pulse injects electrons into the first and second subband of an undoped asymmetric double quantum well (ADQW) with a level spacing smaller than the LO phonon energy. The time evolution of the electron population in these two subbands is monitored by probing the mid-infrared (MIR) intersubband transitions to the empty levels 3 and 4 (Fig.1).

The $Al_{0.25}Ga_{0.75}As$/GaAs ADQW was grown by molecular beam epitaxy on a semi-insulating substrate. It consists of 80 periods of an 80 Å GaAs well and a 90 Å GaAs well, coupled through a 30 Å $Al_{0.}$ Ga $_{.75}$As barrier. The sample was cleaved and polished to a MIR waveguide and mounted on the cold finger of a He continuous flow cryostat (T = 5 K).

The energy levels and wave functions (see Fig. 1) were calculated by solving the Schrödinger equation in the envelope-function formalism. For the spacing between the two lowest electron-subbands we obtain E_{12} = 7.5 meV.

In our time-resolved photoinduced absoption (PIA) setup we use a mode-locked Ti:sapphire laser that delivers 12 fs pulses at a repetition rate of 75 MHz with an average

output power of 850 mW. The laser pulses are centered at a wavelength of 780 nm and the bandwidth is 110 nm (full width at half maximum). Half of the laser intensity served as the visible pump to excite the sample and the other part was focused on a 30 μm thick GaSe crystal to generate a linear polarized MIR probe beam by phase-matched difference frequency mixing [14]. Spectroscopic measurements of the MIR probe were made using an interferometric autocorrelation technique. Details concerning this technique can be found in Ref. 15. An interference filter with 780 nm central wavelength and 30 nm bandwidth was used to select the desired pump-pulse spectrum.

Fig. 2 shows PIA spectra (squares) taken with p-polarized MIR probe pulses at different delay times after excitation. From the excitation power, repetition rate, focus diameter of the pump pulse, and the absorption coefficient of GaAs we estimated a density of photoexcited carriers of $n_S = 8 \times 10^{10}$ cm^{-2}. The spectra exhibit a broad absorption peak around 125-130 meV that clearly shifts to higher energies over time. In addition we observe the onset of a second peak at lower energies that cannot be fully resolved due to the cut-off of our MCT detector.

We explain the blue shift of the high-energy peak by relaxation of the photoexcited electrons from the second to the first subband: 250 ps after excitation the PIA data can be fitted by a single Gaussian of half width at half maximum $\Gamma = 7.5$ meV at an energy of 131 meV (solid line in Fig. 2). This value is in good agreement with the calculated energy for the (1-4) transition and we conclude that 250 ps after the pump all the carriers excited into the second subband are already relaxed to the first subband. At delay times smaller than 250 ps the second subband is populated, and in addition to the (1-4) transition the (2-4) transition also contributes to the PIA spectrum since the

oscillator strength f_{24} is non-zero in an asymmetric structure. For a quantitative analysis we fitted two Gaussian lines (Γ = 7.5 meV) to the experimental curves (dashed and dotted lines in Fig. 2). One line is again at the position of the (1-4) transition, the other 7.5 meV (this is exactly the spacing between levels 1 and 2) below this energy. The monotonous decrease of the area under the (2-4) peak over time is due to a decrease of the (2-4) absorption because of depopulation of the second level. The evolution of the (1-4) peak shows a more complex behavior. First the amplitude rises slightly since the electrons from level 2 add to the electrons in level 1, then it decreases due to carrier recombination. So far we have not discussed the origin of the absorption below 110 meV. From our energy level calculations we expect transitions from the first two subbands to the empty subband 3 at 91.5 meV and 99 meV. Thus we attribute the absorption peak below 110 meV to this transitions. We expect that this peak shows the same time evolution as the high-energy peak and thus gives no additional information about the relaxation processes in the QW.

On the basis of the time-resolved PIA spectra we are able to determine the population dynamics in the QW since the subband population $n_i(t)$ (i = 1,2) is directly proportional to the integrated absorbance: $n_i(t) = K \cdot I_A^{(i-4)} / f_{i4}$, where $I_A^{(i-4)}$ is the area under the peak (i-4), and K is a constant that was chosen such that $n_1(0) + n_2(0) = n_S$ at zero time delay. Fig. 3 presents the electron population of the first and second subband as a function of time delay after optical excitation (squares and circles). About 40 % of the electrons excited by the pump pulse are injected into the second subband. The remaining 60 % are injected into the first subband at a higher k-vector. The electrons in level 2 relax down and add to the carriers in the ground level. This explains why the population $n_1(t)$

rises until 70 ps after the excitation. Subsequently, the carriers recombine and the population drops.

We calculated the temporal evolution of the populations in the two subbands by solving the rate equations for the three-level system shown in Fig. 4. We obtain the following analytical result for the populations in level 1 and 2:

$$n_1(t) = \left[n_1(0) + n_2(0) \cdot \left(1 - \exp(-t / T_{21})\right)\right] \cdot \exp(-t / \tau),$$

$$n_2(t) = n_2(0) \cdot \exp(-t / T_{21}) \cdot \exp(-t / \tau),$$

where T_{21} is the intersubband relaxation time, and τ denotes the recombination time. In our model we have assumed that the recombination time is identical on both subbands. By fitting the calculation (solid and dashed line in Fig. 3) to the experimental data we deduce T_{21} = 100 ps and τ = 410 ps.

In conclusion, we have demonstrated a novel interband pump/intersubband probe technique that directly allows to measure the temporal evolution of the subband populations in semiconductor quantum structures after optical excitation. From these measurements we have determined the intersubband lifetime in a GaAs/AlGaAs ADQW. This technique is especially well suited not only to determine the population dynamics but also to observe gain in structures designed for optical pumping.

This work has been supported by the Fond zur Förderung der Wissenschaftlichen Forschung (SFB-ADLIS).

References

[1] J. Faist, F. Capasso, D. L. Sivco, C. Sirtori, A. L. Hutchinson, and A. Y. Cho, Science 264 (1994) 553.

[2] B. F. Levine, J. Appl. Phys. 74 (1993) R1.

[3] P. Boucaud, F. H. Julien, D. D. Yang, J. M. Lourtioz, E. Rosencher, P. Bois, and J. Nagle, Appl. Phys. Lett. 57 (1990) 215.

[4] K. Craig, C. L. Felix, J. N. Heyman, A. G. Markelz, M. S. Sherwin, K. L. Campman, P. F. Hopkins, and A. C. Gossard, Phys. Rev. Lett 76 (1996) 2382.

[5] K. Craig, C. L. Felix, J. N. Heyman, A. G. Markelz, M. S. Sherwin, K. L. Campman, P. F. Hopkins, and A. C. Gossard, Semicond. Sci. Technol. 9 (1994) 627.

[6] J. N. Heyman, K. Unterrainer, K. Craig, B. Galdrikian, M. S. Sherwin, K. Campman, P. F. Hopkins, and A. C. Gossard, Phys. Rev. Lett. 74 (1995) 2682.

[7] B. N. Murdin, W. Heiss, C. J. G. M. Langerak, S.-C. Lee, I. Galbraith, G. Strasser, E. Gornik, M. Helm, and C. R. Pidgeon, Phys. Rev. B 55 (1997) 5171.

[8] J. N. Heyman, K. Unterrainer, K. Craig, J. Williams, M. S. Sherwin, K. Campman, P. F. Hopkins, A. C. Gossard, B. N. Murdin, and C. J. G. M. Langerak, Appl. Phys. Lett. 68 (1996) 3019.

[9] J. Faist, C. Sirtori, F. Capasso, L. Pfeiffer, and K. W. West, Appl. Phys. Lett. 64 (1994) 872.

[10] M. C. Tatham, J. F. Ryan, and C. T. Foxon, Phys. Rev. Lett. 63 (1989) 1637.

[11] D. Y. Oberli, D. R. Wake, M. V. Klein, J. Klem, T. Henderson, and H. Morkoç, Phys. Rev. Lett. 59 (1987) 696.

[12] M. Hartig, S. Haacke, P. E. Selbmann, B. Deveaud, R. A. Taylor, and L. Rota, Phys. Rev. Lett. 80 (1998) 1940.

[13] J. A. Levenson, G. Dolique, J. L. Oudar, and I. Abram, Phys. Rev. B 41 (1990) 3688.

[14] R. A. Kaindl, D. C. Smith, and T. Elsaesser, Opt. Lett. 23 (1998) 861.

[15] M. Joffre, A. Bonvalet, A. Migus, and J.-L. Martin, Opt. Lett. 21 (1996) 964.

Figure Captions

Figure 1: Energy band diagram of a single period of the $Al_{0.25}Ga_{0.75}As/GaAs$ ADQW structure and squared wave functions. The arrows denote the interband pump and intersubband probe scheme.

Figure 2: Intersubband absorption spectra at four different time delays after the pump (squares) with Gaussian fits for the (1-4) transition (dotted line) and the (2-4) transition (dashed line). The solid line is the sum of the two Gaussians.

Figure 3: Measured (squares and circles) and calculated (lines) population of subbands 1 and 2 as a function of time delay after the excitation.

Figure 4: Three-level system for modeling the subband population dynamics in the QW. T_{21} denotes the intersubband relaxation time, τ is the recombination time.

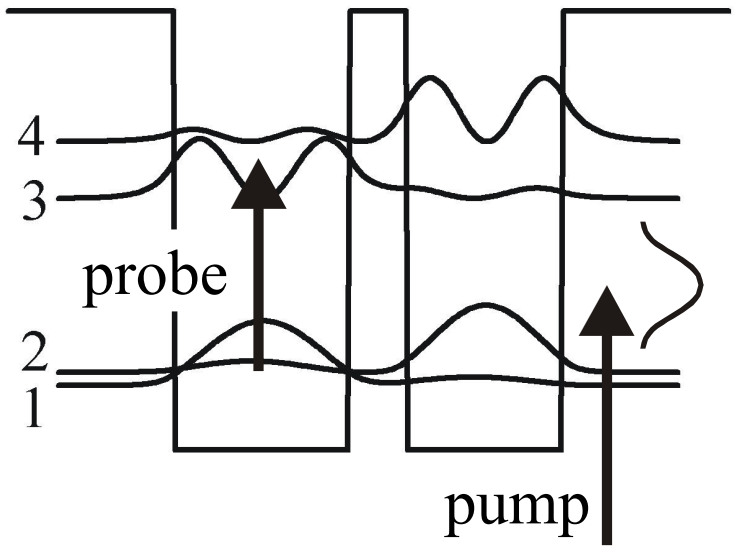
4
3
probe
2
1
pump

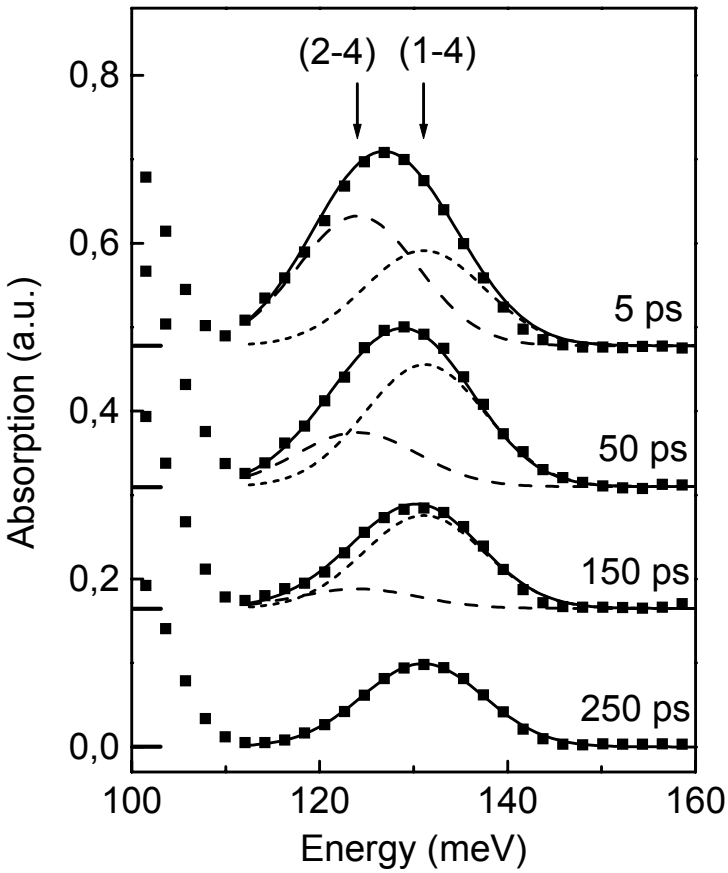
(2-4)
(1-4)
0,8
0,6
0,4
0,2
0,0
Absorption (a.u.)
5 ps
50 ps
150 ps
250 ps
100
120
140
160
Energy (meV)

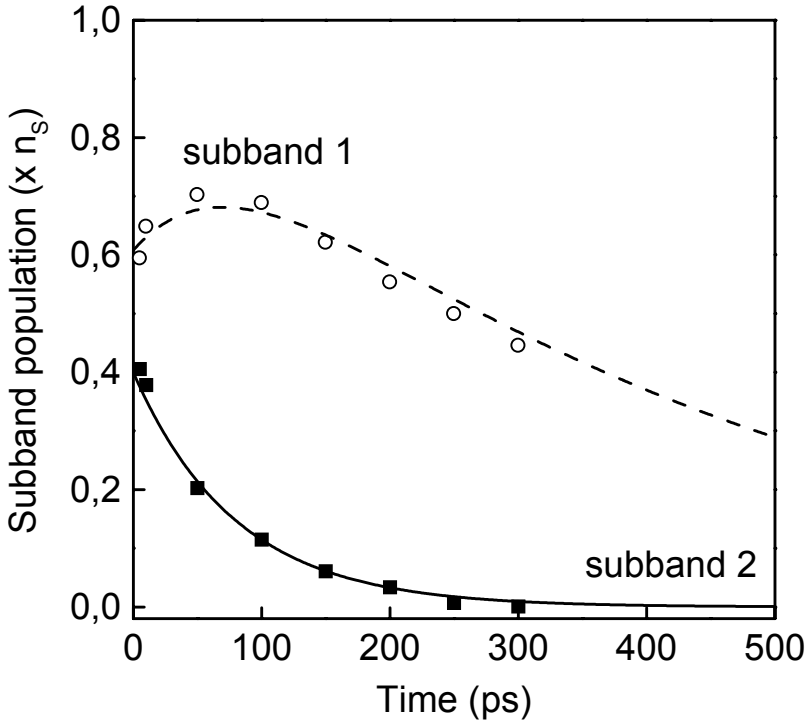
1,0
0,8
0,6
0,4
0,2
0,0
Subband population (x n_s)
subband 1
subband 2
0
100
200
300
400
500
Time (ps)

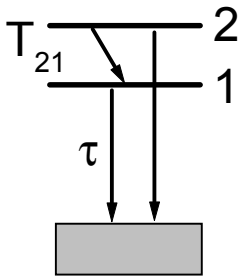
T21
2
1
τ